MOLECULAR AND CELLULAR BIOLOGY, Dec. 2008, p. 7236–7244 Vol. 28, No. 23
0270-7306/08/$08.00+0 doi:10.1128/MCB.01334-08

Laforin Negatively Regulates Cell Cycle Progression through Glycogen Synthase Kinase 3β-Dependent Mechanisms▽§

Runhua Liu,[1] Lizhong Wang,[1] Chong Chen,[1] Yan Liu,[1] Penghui Zhou,[1] Yin Wang,[1] Xirui Wang,[1] Julie Turnbull,[4] Berge A. Minassian,[4] Yang Liu,[1,2] and Pan Zheng[1,3]*

Division of Immunotherapy, Department of Surgery, Program of Molecular Mechanism of Diseases and Comprehensive Cancer Center,[1] Division of Molecular Medicine and Genetics, Department of Internal Medicine,[2] and Department of Pathology,[3] University of Michigan, Ann Arbor, Michigan 48109, and Program in Genetics and Genome Biology, The Hospital for Sick Children, Toronto, Ontario, Canada[4]

Received 21 August 2008/Accepted 19 September 2008

Glycogen synthase kinase 3β (GSK-3β) represses cell cycle progression by directly phosphorylating cyclin D1 and indirectly regulating cyclin D1 transcription by inhibiting Wnt signaling. Recently, we reported that the *Epm2a*-encoded laforin is a GSK-3β phosphatase and a tumor suppressor. The cellular mechanism for its tumor suppression remains unknown. Using ex vivo thymocytes and primary embryonic fibroblasts from *Epm2a*$^{-/-}$ mice, we show here a general function of laforin in the cell cycle regulation and repression of cyclin D1 expression. Moreover, targeted mutation of *Epm2a* increased the phosphorylation of Ser9 on GSK-3β while having no effect on the phosphorylation of Ser21 on GSK-3α. In the GSK-3β$^{+/+}$ but not the GSK-3β$^{-/-}$ cells, *Epm2a* small interfering RNA significantly enhanced cell growth. Consistent with an increased level of cyclin D1, the phosphorylation of retinoblastoma protein (Rb) and the levels of Rb-E2F-regulated genes *cyclin A*, *cyclin E*, *MCM3*, and *PCNA* are also elevated. Inhibitors of GSK-3β selectively increased the cell growth of *Epm2a*$^{+/+}$ but not of *Epm2a*$^{-/-}$ cells. Taken together, our data demonstrate that laforin is a selective phosphatase for GSK-3β and regulates cell cycle progression by GSK-3β-dependent mechanisms. These data provide a cellular basis for the tumor suppression activity of laforin.

Cell cycle progression is facilitated by cyclin-dependent kinases (CDKs) that are activated by cyclins, including cyclin D1, and inhibited by CDK inhibitors (27, 29). Cyclin D1 is a critical regulator involved in cell cycle progression through the G_1 phase and into the S phase (18, 33). The active cyclin D1/CDK4 complex initiates the phosphorylation of retinoblastoma protein (Rb) (9), which disrupts Rb-mediated transcriptional repression of E2F and facilitates cell cycle progression (27, 29). However, the activity of cyclin D1/CDK4 is specifically inhibited by four INK4 proteins ($p^{16INK4a}$, $p^{15INK4b}$, $p^{18INK4c}$, and $p^{19INK4d}$) (13, 14, 34) and by glycogen synthase kinase 3β (GSK-3β) (3, 7). GSK-3β phosphorylates cyclin D1 at Thr286 (3, 7) and thereby triggers its nuclear export, ubiquitination, and proteasomal degradation (7).

GSK-3β is a multifunctional serine/threonine protein kinase (2, 6, 12) and a component of multiple signal transduction pathways, including the insulin, Wnt, and Ras signaling pathways. In the Wnt signaling pathway, GSK-3β phosphorylates β-catenin for its degradation and is an essential negative regulator of the Wnt/β-catenin pathway (1, 4). Wnt inhibits the enzymatic activity of GSK-3β, thereby stabilizing β-catenin and enabling its association with T-cell factor (TCF)/lymphoid enhancer-binding factor (LEF) protein complexes to activate the transcription of target genes, including those like c-*myc* and *cyclin D1* (25). However, how GSK-3β activity is regulated has been poorly understood.

Epm2a encodes a 331-amino-acid dual-specificity phosphatase called laforin (5, 10, 20–22). Loss-of-function mutations in *Epm2a* result in Lafora disease, an autosomal recessive disorder in which glycogen metabolism is disturbed, resulting in the formation of insoluble forms of glycogen and their precipitation and accumulation in neurons, with subsequent neurodegeneration and epilepsy (22). Recently, we demonstrated that laforin causes the dephosphorylation of GSK-3β at Ser9 (17, 32) and maintains its steady-state activity (32). More importantly, we showed that the absence of laforin results in neoplastic transformation and, in an immunocompromised host, in tumor formation and metastasis. We showed that laforin's tumor suppressor effect is in part mediated through its action on GSK-3β in the Wnt signaling pathway (32). Interestingly, how laforin represses tumor development remains largely unexplained. Based on the laforin–GSK-3β connection, it is plausible that laforin may regulate GSK-3β-mediated degradation of cyclin D1 and/or modulate its transcription via the β-catenin–TCF complex. Here, we report that, by a strict GSK-3β-dependent mechanism, laforin negatively regulates cell cycle progression and modulates the levels of cyclin D1. These data provide a missing link between laforin and cell cycle regulation and explain at least in part the tumor suppressor function of laforin.

MATERIALS AND METHODS

Mice. *Epm2a*$^{-/-}$ mice and their wild-type (WT) littermates have been described in full (11). The mice were housed in the University of Michigan animal facility, and animal protocols were reviewed and approved by the University of

* Corresponding author. Mailing address: Department of Surgery, 1810 BSRB, 109 Zina Pitcher Place, University of Michigan, Ann Arbor, MI 48109. Phone: (734) 615-3464. Fax: (734) 763-2162. E-mail: panz@umich.edu.

§ Supplemental material for this article may be found at http://mcb.asm.org/.

▽ Published ahead of print on 29 September 2008.

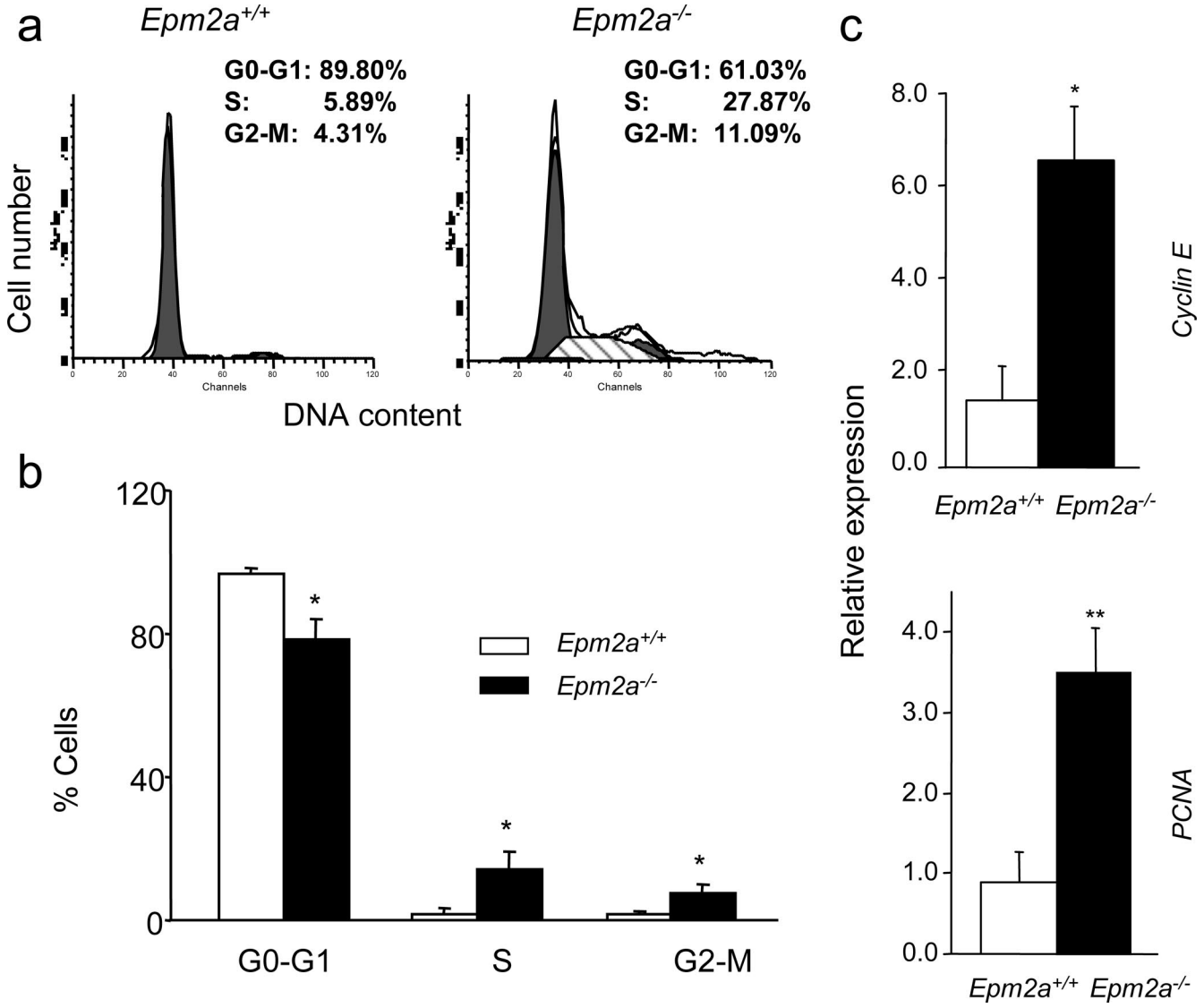

FIG. 1. Targeted mutation of *Epm2a* increases the proportion of thymocytes in the cycle. (a and b) The percentages of cells in G_0/G_1, S, and G_2/M phases were evaluated by flow cytometry. A representative profile from each group (a) and the summary data (b) are shown. The experiments whose data are shown in this figure were repeated three times, involving a total of seven mice in each group. (c) *Epm2a* downregulates the mRNA levels of *cyclin E* and *PCNA*. Data shown are relative transcript levels after normalization against the housekeeping gene *Hprt*. The transcript levels in one of the WT mice were artificially defined as 1.0. Data shown are means ± SD from three independent experiments. *, $P < 0.05$; **, $P < 0.01$.

Michigan Institutional Animal Care and Use Committee. The WT and *Epm2a*$^{-/-}$ murine embryonic fibroblasts (MEF) were prepared based on an established procedure (8). GSK-3β$^{+/+}$ and GSK-3β$^{-/-}$ MEF were obtained from James R. Woodgett (15).

***Epm2A* siRNA constructs.** Oligonucleotides encoding two small interfering RNAs (siRNAs) directed against *Epm2a* have core sequences as follows: siRNA1, 5′-AAGGTGCAGTACTTCATCATG-3′, and siRNA2, 5′-GGTTCA CTCTTCCATATGC-3′. These oligonucleotides were inserted into a modified pLenti6/V5-D-TOPO vector (Invitrogen). Lentivirus stocks were produced in 293FT cells according to the manufacturer's protocol. Virally transduced cells were selected with blasticidin.

Colony formation assay. GSK-3β$^{+/+}$ or GSK-3β$^{-/-}$ cells were transfected with either the control vector or vectors that express *Epm2a* siRNAs as described previously (32). At 48 h after transduction, cells were counted and plated in 100-mm dishes in triplicate and cultured in medium containing 5 μg/ml blasticidin. After 3 weeks in culture, the colonies were stained with 0.125% crystal violet, and the total number of colonies (≥20 cells) per plate was counted using a microscope.

Cell growth assay. Cells were seeded into 12-well plates at a density of 1.5×10^4 cells/well and were grown in complete medium containing 10% fetal bovine serum (FBS) as described above. The viable cells were stained by 0.4% trypan blue solution (Sigma), and the cells were counted in triplicate every day using a hemocytometer.

Serum starvation. The cells were seeded into six-well plates at 3×10^5 cells/well in Dulbecco modified Eagle medium (DMEM) without FBS for 24 h. After reseedings with medium containing 10% FBS, cells were collected every 8 h for up to 24 h for analyses by flow cytometry, real-time PCR, and Western blotting.

Cell cycle analysis. The cell monolayer was harvested after treatment with EDTA-trypsin, washed with ice-cold phosphate-buffered solution (PBS), and fixed in ice-cold 70% ethanol overnight at −30°C. After being washed twice with PBS, the cells were incubated in RNase A-PBS (100 μg/ml) at 37°C for 30 min. DNA was labeled with propidium iodide (50 μg/ml) (BD Biosciences) and analyzed with an LSII flow cytometer and CELLQuest software (Becton Dickinson). The percentages of cells in G_0/G_1, S, and G_2/M phases were evaluated by analyzing 2×10^4 cells using the ModFit LT 3.0 program (Becton Dickinson).

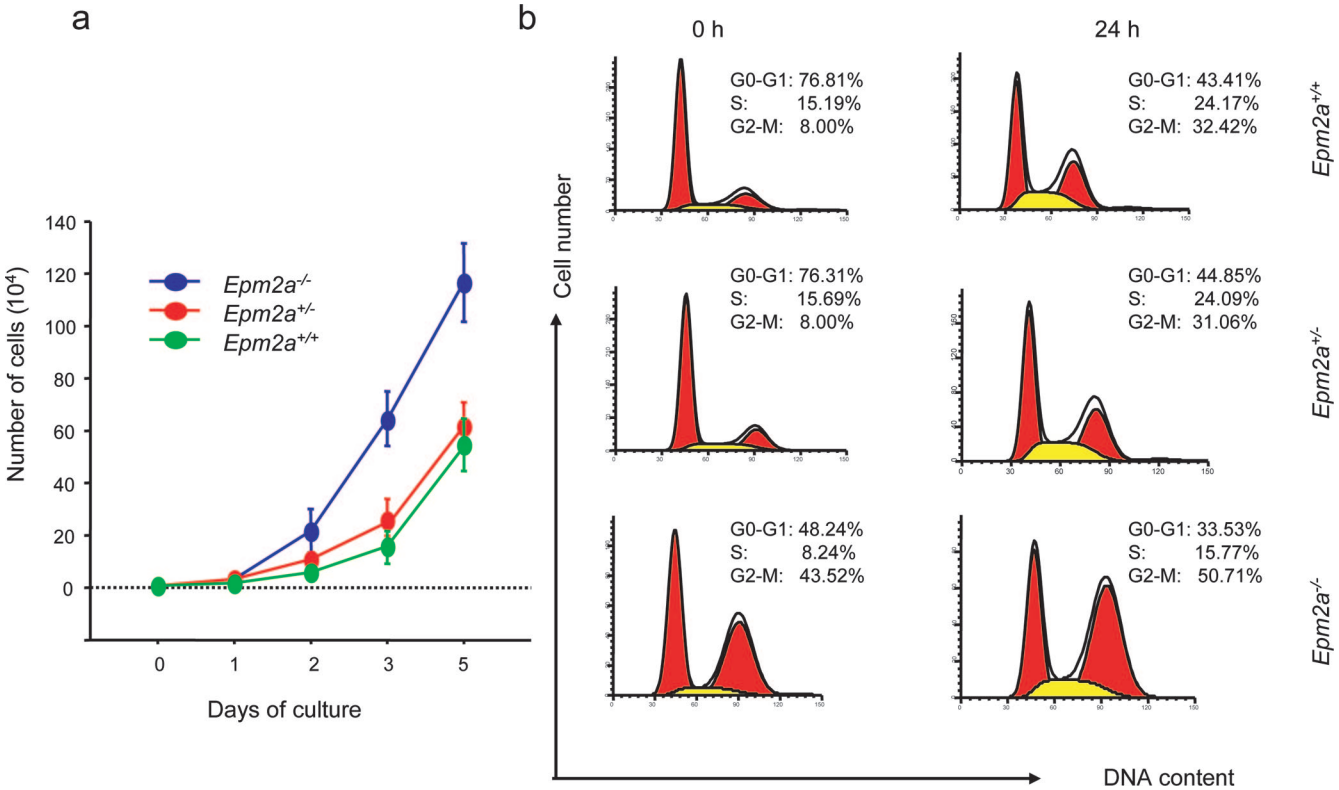

FIG. 2. *Epm2a* inhibited cell growth. (a) Growth rate. Equal numbers (1.0×10^4 cells/well) of MEF from $Epm2^{+/+}$, $Epm2^{+/-}$, and $Epm2a^{-/-}$ mouse embryos were seeded on 12-well plates and cultured with DMEM with 10% FBS for 0 to 5 days. The cells were treated with trypsin, and the number of viable cells was counted with a hemocytometer. Data are shown as means and SD from experiments with three independent embryos. (b) The MEF prepared from $Epm2^{+/+}$, $Epm2^{+/-}$, and $Epm2a^{-/-}$ embryos were incubated for 24 h with FBS-free medium to synchronize cells in G_0/G_1 phase (0 h). After the cells were shifted to the medium with 10% FBS for 24 h, they were collected for analysis (24 h). The percentages of cells in G_0/G_1, S, and G_2/M phases were evaluated by flow cytometry. The experiments whose data are shown in this figure were repeated three times, involving a total of three embryos in each group.

Real-time reverse transcription-PCR. Total RNA was isolated from the GSK-$3\beta^{+/+}$ and GSK-$3\beta^{-/-}$ cells using the QIAamp RNA minikit (Qiagen). All RNA samples were treated with DNase I to eliminate any residual DNA. We performed first-strand cDNA synthesis using the SuperScript first-strand synthesis system kit (Invitrogen) and analyzed the resulting cDNA for differential gene expression by using real-time PCR in the Applied Biosystems 7900HT fast real-time PCR system using a Sybr green PCR master mix kit (Applied Biosystems). All primer sequences are listed in Table S1 in the supplemental material. The relative amounts of gene expression were calculated by using the expression of *Hprt* as an internal standard.

Western blotting. Single-cell suspensions were lysed in ice-cold buffer (20 mM Tris-HCl [pH 7.5], 150 mM NaCl, 1 mM EDTA, 1 mM EGTA, 1% Triton X-100, 2.5 mM sodium pyrophosphate, 1 mM β-glycerophosphate, 1 mM sodium fluoride, and 1 mM sodium orthovanadate supplemented with complete protease and phosphatase inhibitors [Sigma]).

For nuclear proteins, the cells were first incubated in buffer A (10 mmol/liter HEPES [pH 7.8], 10 mmol/liter KCl, 2 mmol/liter $MgCl_2$, 0.1 mmol/liter EDTA, 1% NP-40, and protease inhibitors), and the pellet was suspended in buffer B (50 mmol/liter HEPES [pH 7.8], 300 mmol/liter NaCl, 50 mmol/liter KCl, 0.1 mmol/liter EDTA, 10% [vol/vol] glycerol, and protease inhibitors). The lysates were collected by centrifugation at 4°C at 13,000 rpm for 10 min. Aliquots of the supernatants containing 50 μg of protein were resolved by electrophoresis and transferred to a Hybond-P (polyvinylidene difluoride) membrane (Amersham Biosciences). The primary antibodies were antilaforin (Genemed Synthesis, Inc., San Francisco, CA), anti-GSK-3β (Cell Signaling), anti-phospho-GSK-3β (Ser9) (catalog no. 9336; Cell Signaling), anti-Akt (9272; Cell Signaling), anti-phospho-Akt (Ser473) (9271; Cell Signaling), anti-cyclin D1 (sc-753; Santa Cruz Biotechnology), phospho-cyclin D1 (Thr286) (2921; Cell Signaling), anti-CDK4 (2906; Cell Signaling), anti-phospho-Rb (Ser795) (9301; Cell Signaling), anti-β-catenin (9587; Cell Signaling), and anti-β-actin (A5441; Sigma) antibodies. The secondary antibodies were anti-rabbit or -mouse immunoglobulin G-horseradish peroxidase (7074 or 7076; Cell Signaling). The signals were detected by enhanced chemiluminescence reagents (Amersham Biosciences).

MTT assay. Cell proliferation was detected by 3-(4,5-dimethylthiazol-2-yl)-2,5-diphenyl tetrazolium bromide (MTT) (Sigma) assay. Briefly, when cells were in exponential growth, they were seeded on a 96-well plate (2×10^4 cells/100 ml/well) for 24 h until confluence occurred. Cells were divided into a control (dimethyl sulfoxide) group, a lithium chloride (LiCl) (L9650; Sigma) group, and a 6-bromoindirubin-3′-oxime (BIO) (B1686; Sigma) group. The concentration of LiCl was 25 mM, and that of BIO was 1 μM. After 48 h, 10 μl MTT (5 mg/ml) was added and the mixture was incubated at 37°C for 4 h. Dimethyl sulfoxide (200 μl) was added to each well, and the plate was oscillated for 10 min until the crystals were dissolved completely. Absorbance (optical density) was measured at 570 nm with a scanning multiwell spectrophotometer (BioTek Instruments Inc., Burlington, VT).

Statistics. Differences in levels of gene expression and numbers of colonies were evaluated by using the unpaired Student *t* test, and values are represented by means ± standard deviations (SD). The comparisons between cell growth curves of silencing and control groups were made by using Fisher's protected least-significant-difference test. StatView 5.0 software (SAS Institute Inc.) was used for all statistical calculations.

RESULTS

Targeted mutation of *Epm2a* promotes cell cycle progression under physiological conditions. To determine whether Epm2a deficiency alters the cell cycle in vivo, we compared ex vivo thymocytes from WT mice to those with a targeted dele-

tion of the phosphatase domain of laforin (11). As shown in Fig. S1 in the supplemental material, this mutation does not significantly affect the differentiation of thymocytes, as judged both by the normal number of $CD3^+$ cells in the thymus and by the normal distribution of CD4- and CD8-expressing cells. The comparable distributions of thymocyte subsets allowed us to compare the cell cycles independently of their potential effect on cellular differentiation. As shown in Fig. 1a and b, deletion of the phosphatase domain of the *Epm2a* gene resulted in a significant increase in the numbers of cells at the S and G_2/M phases. Correspondingly, the transcript levels of *cyclin E* and *PCNA* were also substantially increased (Fig. 1c). These results confirmed that *Epm2a* is a negative regulator of the cell cycle under physiological conditions. Nevertheless, despite the more rapid progression of the cell cycle, we did not observe a significant increase in the number of thymocytes (data not shown). Therefore, it is likely that other mechanisms operated to control the total number of thymocytes, even when the cell cycle was dysregulated.

To substantiate this observation, we prepared MEF from WT and $Epm2a^{-/-}$ mice and compared their growth rates. As shown in Fig. 2a, the $Epm2a^{-/-}$ MEF grew significantly faster than the $Epm2a^{+/+}$ and $Epm2a^{+/-}$ MEF. Interestingly, cell cycle analysis indicated that while the overwhelming majority of the $Epm2a^{+/+}$ and $Epm2a^{+/-}$ MEF rested at the G_0/G_1 phase under the condition of serum starvation, the majority of the $Epm2a^{-/-}$ MEF, cultured side by side under the same condition, were at the S and G_2/M phases (Fig. 2b). Twenty-four hours after being supplied serum, high percentages of S and G_2/M cells were still observed in the $Epm2a^{-/-}$ MEF. Taken together, our data demonstrated that targeted mutation and siRNA silencing of the *Epm2a* gene promoted cell growth. Therefore, laforin is an important negative regulator for cell cycle progression.

The targeted mutation of *Epm2a* selectively increases the phosphorylation of GSK-3β as well as the expression of cyclin D1. In order to understand the mechanism by which the targeted mutation of *Epm2a* promotes cell cycle progression, we first compared the levels of phosphorylation of GSK-3β in primary MEF prepared from WT and $Epm2a^{-/-}$ embryos. As shown in Fig. 3, GSK-3β phosphorylation at the Ser9 position was dramatically increased in the $Epm2a^{-/-}$ MEF. In contrast, no increase was found in the phosphorylation of Ser21 in GSK-3α. Thus, laforin is a selective phosphatase for GSK-3β. The selectivity of laforin allows differential regulation of the two similar enzymes.

Since cyclin D1 is a known substrate for GSK-3β, we tested the role of *Epm2a* in the protein levels and phosphorylation of cyclin D1. As shown in Fig. 3, the expression of cyclin D1 was substantially increased in $Epm2a^{-/-}$ cells. This increase was likely due, at least in part, to decreased GSK-3β function, as the phosphorylation of cyclin D1 was significantly reduced.

***Epm2a* silencing accelerates the growth of MEF in a GSK-3β-dependent fashion.** Since GSK-3β is a substrate for laforin, a natural question is whether laforin-mediated growth inhibition is mediated by GSK-3β. We took a genetic approach to address this issue.

We transduced MEF with a lentivirus vector containing the blasticidin resistance gene in conjunction with or without *Epm2a* siRNA. The drug-resistant clones were screened for *Epm2a* expression by real-time PCR. Multiple independent *Epm2a*-silenced clones with a >10-fold reduction in the level of *Epm2a* mRNA were chosen for the study. As shown in Fig. 4a, relative to *Hprt* levels, a representative *Epm2a*-silenced clone had about a 20-fold reduction in the *Epm2a* mRNA level in comparison to those in the vector-transduced clones. Drastic reduction in the level of the laforin protein was also observed (Fig. 4b). Consistent with the GSK-3β phosphatase activity of laforin (32), GSK-3β is hyperphosphorylated in the *Epm2a*-silenced cell line in comparison with its level of phosphorylation in the vector-transduced cell line.

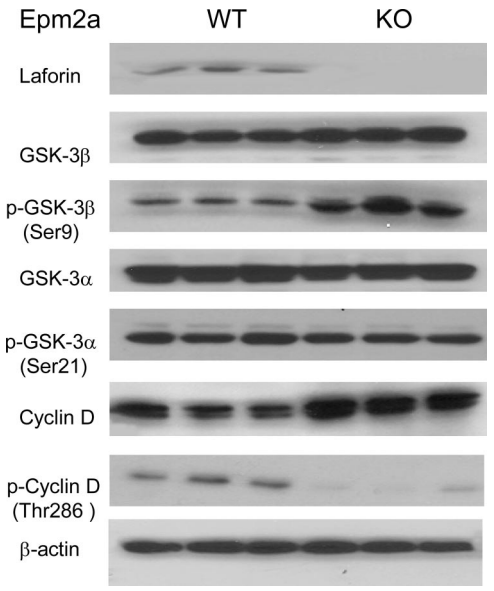

FIG. 3. Targeted mutation of *Epm2a* increased the phosphorylation of cyclin D1 and GSK-3β but not GSK3α. Primary MEF from three WT and three *Epm2a* embryos were serum starved for 24 h and restimulated with 10% fetal calf serum for 24 h. The lysates were analyzed by Western blotting for their levels of laforin, GSK-3β, phospho-GSK-3β [p-GSK-3β (Ser9)], GSK-3α, phospho-GSK3α [p-GSK3α (Ser21)], cyclin D1, and phospho-cyclin D1 [p-cyclin D1 (Thr 286)], with β-actin as a loading control. The experiments whose data are shown in this figure were repeated four times. KO, knockout.

As the first test of the function of laforin in cell growth, we monitored the growth rate of control and *Epm2a*-silenced cell lines at days 1 to 6 after plating. Figure 4c shows summary data of five representative clones from each group. The cell numbers of *Epm2a*-silenced clones were significantly higher than that of control cells from day 2 to day 6. Fisher's protected least-significant-difference test revealed a very significant difference between the cell growth curves of silenced and control cells ($P < 0.0001$). To confirm the effect of *Epm2a* in cell growth, we transfected the siRNA and control vectors into the MEF. The number of drug-resistant clones was used as the parameter for cell growth. As shown in Fig. 4d, almost 10-fold-more drug-resistant clones were observed in the *Epm2a*-silenced clone than in the control cells. Thus, siRNA silencing of *Epm2a* substantially increased the growth of MEF.

In parallel with the above-described experiments using WT GSK-$3\beta^{+/+}$ MEF, we also silenced *Epm2a* in the MEF derived from the GSK-$3\beta^{-/-}$ littermate mice. As shown in Fig. 4e, in comparison to what occurred with control clones transduced

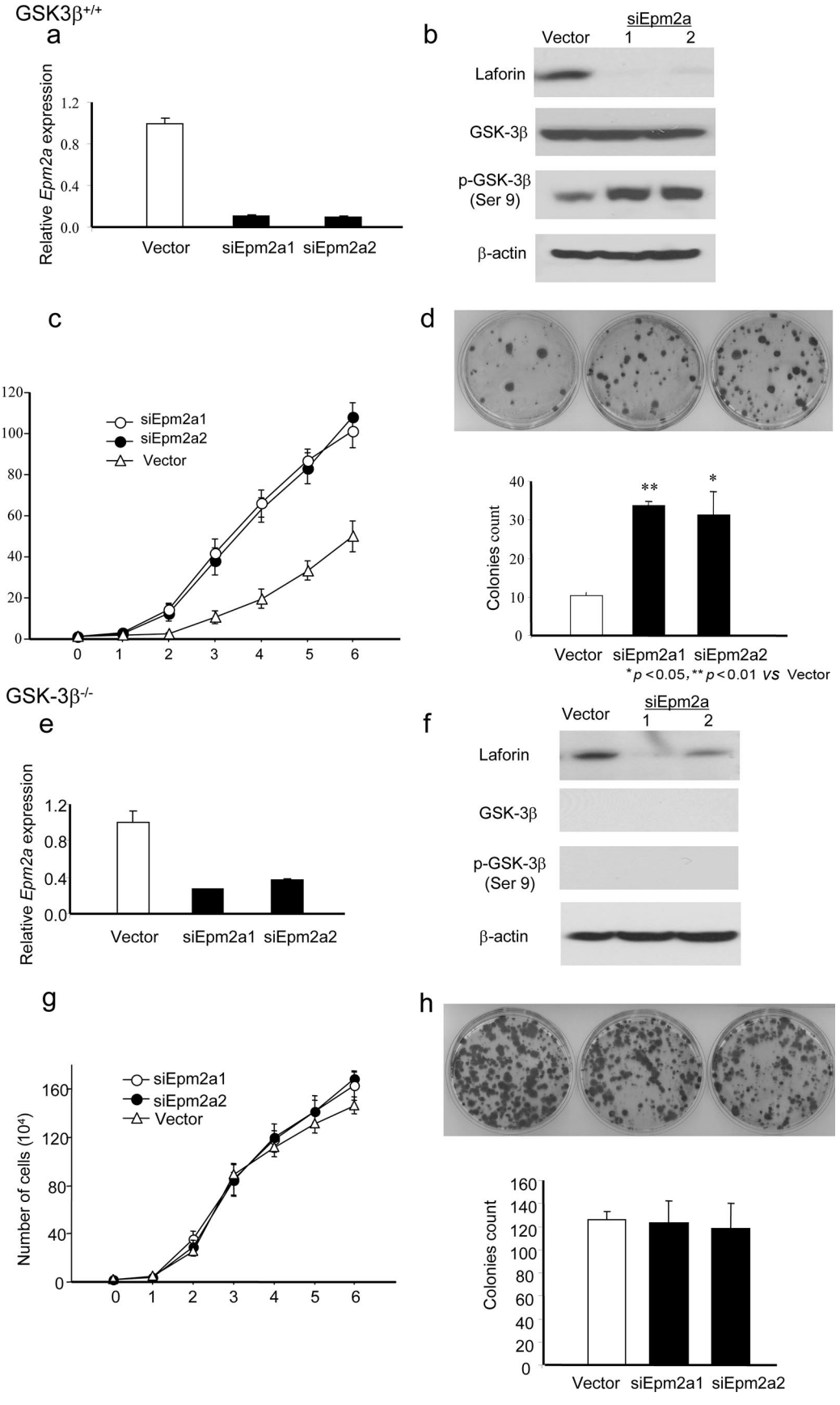
GSK3β+/+
a
Relative Epm2a expression
1.2
0.8
0.4
0.0
Vector
siEpm2a1
siEpm2a2
b
siEpm2a
Vector
1
2
Laforin
GSK-3β
p-GSK-3β (Ser 9)
β-actin
c
Number of cells (10⁴)
120
100
80
60
40
20
0
0 1 2 3 4 5 6
siEpm2a1
siEpm2a2
Vector
d
Colonies count
40
30
20
10
0
**
*
Vector siEpm2a1 siEpm2a2
*p < 0.05, **p < 0.01 vs Vector
GSK-3β-/-
e
Relative Epm2a expression
1.2
0.8
0.4
0.0
Vector
siEpm2a1
siEpm2a2
f
siEpm2a
Vector
1
2
Laforin
GSK-3β
p-GSK-3β (Ser 9)
β-actin
g
Number of cells (10⁴)
160
120
80
40
0
0 1 2 3 4 5 6
siEpm2a1
siEpm2a2
Vector
h
Colonies count
160
140
120
100
80
60
40
20
0
Vector siEpm2a1 siEpm2a2

TABLE 1. GSK-3β-dependent regulation of cell cycle progression by laforin[a]

Cell type	Length of culture with medium (h)	siRNA	% of cells (mean ± SD) in indicated phase[b]		
			G_0/G_1	S	G_2/M
GSK-3β$^{+/+}$	0	Control	90.9 ± 4.7	6.3 ± 3.3	2.5 ± 1.4
		Epm2a silenced	90.0 ± 3.2	7.9 ± 1.9	2.0 ± 1.8
	8	Control	81.8 ± 1.7	11.9 ± 0.8	6.3 ± 0.9
		Epm2a silenced	76.5 ± 3.2	17.3 ± 2.9*	6.2 ± 1.2
	16	Control	70.4 ± 2.8	19.3 ± 2.7	10.3 ± 1.5
		Epm2a silenced	56.9 ± 2.8*	37.1 ± 3.6*	6.1 ± 0.5
	24	Control	45.2 ± 2.3	47.2 ± 2.6	7.6 ± 1.5
		Epm2a silenced	44.9 ± 1.3	16.5 ± 3.5*	38.6 ± 4.3**
GSK-3β$^{-/-}$	0	Control	83.6 ± 1.9	11.7 ± 1.8	4.7 ± 1.1
		Epm2a silenced	82.4 ± 2.6	11.2 ± 0.6	6.4 ± 2.3
	8	Control	78.9 ± 1.3	14.8 ± 1.1	6.3 ± 0.2
		Epm2a silenced	78.0 ± 0.7	15.9 ± 1.2	6.1 ± 0.5
	16	Control	57.0 ± 1.0	36.9 ± 3.0	6.1 ± 3.4
		Epm2a silenced	57.5 ± 2.2	35.0 ± 3.5	6.3 ± 3.1
	24	Control	31.5 ± 1.8	31.6 ± 0.3	36.9 ± 1.5
		Epm2a silenced	34.4 ± 0.9	30.9 ± 5.6	34.7 ± 5.0

[a] The *Epm2a*-silenced and control cells were incubated for 24 h in FBS-free medium to synchronize cells in the G_0/G_1 phase at 0 h. The cells then were incubated in medium with 10% FBS and collected at 8 h, 16 h, and 24 h.

[b] The percentages of cells in G_0/G_1, S, and G2/M phases were evaluated by flow cytometry. Data shown are from representative clones from each group. At least three clones in each group were tested, and each clone had been tested at least three times. *, $P < 0.05$; **, $P < 0.01$ versus the control group.

with the vector alone, siRNA reduced *Epm2a* by more than 60 to 80%. Likewise, a substantial reduction in the laforin protein was also observed (Fig. 4f). Side-by-side analysis of both the growth curve (Fig. 4g) and colony formation capacity (Fig. 4 h) indicated that *Epm2a* silencing had no effect on the growth of GSK-3β$^{-/-}$ MEF. These results demonstrated that *Epm2a*-mediated growth inhibition strictly depended on GSK-3β.

A potential caveat of comparing WT and GSK-3β$^{-/-}$ cell lines is that the difference reported above may not be related to targeted mutation of GSK-3β. To address this issue, we reconstituted the GSK-3β$^{-/-}$ cell line with GSK-3β or the control vector. As shown in Fig. S2 in the supplemental material, reconstitution of GSK-3β restored the cellular response to siRNA silencing of *Epm2a*. Therefore, the difference observed between the GSK3-β$^{+/+}$ and GSK-3β$^{-/-}$ cell lines can be attributed to GSK-3β.

To test whether *Epm2a*'s effects on cell cycle progression depend on GSK-3β, we examined the cell cycle in MEF lines by using flow cytometry with propidium iodide staining. As shown in Table 1, at 24 h after serum starvation, approximately 90% of the WT cells were at rest in the G_0/G_1 phase and less than 7% of the cells were at the S phase, regardless of their *Epm2a* status. When the cells were cultured with medium containing 10% FBS for 8 h, 17.3% of the *Epm2a*-silenced cells entered the S phase while only 11.9% of the vector-transduced cells entered the S phase. The difference was more remarkable at 16 h, when 37.1% of the *Epm2a*-silenced cells and 19% of the vector-transduced cells entered S phase. By 24 h, when 47.2% of the vector-transduced cells entered the S phase, many of the *Epm2a*-silenced cells had reached the G_2/M phase. However, *Epm2a* silencing made no difference in the cell cycle progression of GSK-3β$^{-/-}$ cells. Thus, *Epm2a* is a negative

FIG. 4. siRNA silencing of *Epm2a* promoted the growth of GSK-3β$^{+/+}$ (a to d) but not GSK-3β$^{-/-}$ (e to h) MEF. (a and e) mRNA levels of *Epm2a* in *Epm2a*-silenced cells (siEpm2a1 and siEpm2a2) (black bars) and control cells (white bars). Data shown are relative amounts of transcripts after normalization against the amounts of total RNA based on the levels of *Hprt* mRNA. The mean with the control vector is artificially defined as 1.0. Data represent the means ± SD from triplicate samples and are representative of three to five clones used in the study. (b and f) Levels of laforin, GSK-3β, and phospho-GSK-3β [p-GSK-3β (Ser9)] from *Epm2a*-silenced and control GSK-3β$^{+/+}$ (b) or GSK-3β$^{-/-}$ (f) cells by Western blot analysis. (c and g) Impact of *Epm2a* silencing on the growth of GSK-3β$^{+/+}$ (c) or GSK-3β$^{-/-}$ (g) MEF. Equal numbers (1.5×10^4 cells/well) of *Epm2a*-silenced and control cells were seeded on 12-well plates and cultured with DMEM with 10% FBS for 0 to 6 days. The cells were treated with trypsin, and the number of viable cells was counted with a hemocytometer. Data shown were means and SD from five independent clones per group. (d and h) Colony formation assay for the effect of *Epm2a* siRNAs GSK-3β$^{+/+}$ (d) or GSK-3β$^{-/-}$ (h) MEF. At 48 h after transfection with either the control vector or siRNA-expressing plasmids, the cells were trypsinized and plated in 100-mm dishes (1×10^4 cells per dish) and cultured in medium containing 5 μg/ml blasticidin. After 3 weeks, the cells were stained with crystal violet. Photographs of the cells are shown (d and h [top]), while the total number of colonies (≥20 cells) per plate (for each of the three plates) was counted under a microscope. Data represent the means ± SD from triplicate plates. The testing for these data was repeated at least three times.

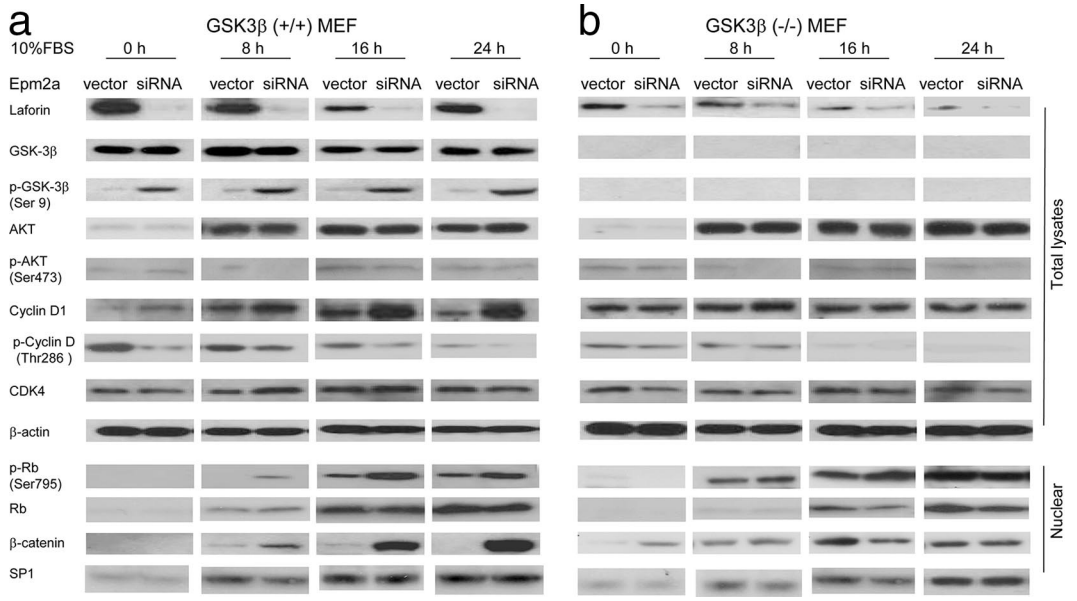

FIG. 5. The *Epm2a*-silenced cells upregulated cyclin D1 and increased Wnt signaling in GSK-3β$^{+/+}$ MEF (a) but not in GSK-3β$^{-/-}$ MEF (b). The *Epm2a*-silenced and control cells were left hungry for 24 h without FBS (0 h). After serum starvation, the synchronized cells were incubated with 10% FBS for 8 h, 16 h, and 24 h. Then, these cells were harvested for Western blotting to determine their amounts of laforin, GSK-3β, phospho-GSK-3β [p-GSK-3β (Ser 9)], Akt, phospho-AKT [p-AKT (Ser473)], cyclin D1, phospho-cyclin D1 [p-cyclin D1 (Thr 286)], CDK4, β-actin, phospho-Rb [p-Rb (Ser795)], Rb, β-catenin, and SP1 antibodies. This experiment was repeated three times.

regulator for cell cycle progression. The more rapid progression explains the more rapid cell growth in the *Epm2a*-silenced cells.

***Epm2a* regulates the expression of cyclin D1 by GSK-3β-dependent mechanisms.** Given the important role of cyclin D1 in the G_1/S transition (24, 33), we tested the role of *Epm2a* in the expression of cyclin D1 in the GSK-3β$^{+/+}$ and GSK-3β$^{-/-}$ cell lines. The function of cyclin D1 was evaluated by the phosphorylation of Rb. The MEF were starved in serum-free medium for 24 h. At 0, 8, 16, and 24 h after culturing in 10% FBS-containing medium, the total cellular or nuclear lysates were isolated and subjected to Western blot analysis. As shown in Fig. 5a, although GSK-3β expression was not changed after the serum stimulation, phospho-GSK-3β (Ser9) was increased. Importantly, the increase was much greater in the *Epm2a*-silenced cells than in those transduced with control lentivirus. The increased phosphorylation confirmed the functional silencing of *Epm2a*. Importantly, the expression of cyclin D1 was dramatically increased in *Epm2a*-silenced cells after the serum stimulation. For the control, expression of Akt and CDK4 was unaffected by the *Epm2a* siRNA. Importantly, since the levels of cyclin D1 were observed in the siRNA-silenced GSK-3β$^{-/-}$ cell line (Fig. 5b), the function of the *Epm2a* gene is likely GSK-3β dependent.

It is established that cyclin D1 and CDK4 together form an Rb kinase (9, 18); therefore, we isolated the nuclear extract and tested the phosphorylation of Rb at position Ser795. As shown in Fig. 5a (bottom panels), *Epm2a* siRNA significantly increased phosphorylated Rb in the nuclear extract. This effect was not observed in the GSK-3β$^{-/-}$ cells (Fig. 5b).

To determine the functional significance of the cyclin D1-Rb signaling pathway, we evaluated the impact of the *Epm2a* siRNA on the transcript levels of Rb-E2F target genes. In the GSK-3β$^{+/+}$ cells, the mRNA expression levels of E2F target genes such as *cyclin A*, *cyclin E*, *MCM3*, and *PCNA* (16, 23, 25, 26) were significantly higher in *Epm2a*-silenced cells than those in control cells after 10% FBS stimulation for 16 h (Fig. 6a). In the GSK-3β$^{-/-}$ cells, however, there were no significant differences in the levels of target gene expression between *Epm2a*-silenced and control groups (Fig. 6b). Therefore, the cyclin D1-Rb pathway likely plays a significant role in laforin-mediated cell cycle regulation. To substantiate this notion, we also compared the levels of *cyclin E* and *PCNA* in the WT and the *Epm2a*$^{-/-}$ thymocytes. As shown in Fig. 1c, targeted mutation of *Epm2a* resulted in 5.5-fold and 2.5-fold increases in *cyclin E* and *PCNA*, respectively. Thus, the *Epm2–GSK-3*β-regulated cyclin D1-Rb pathway significantly affects the expression of genes with important functions in cellular growth.

Targeted mutation of *Epm2a* abrogates growth promotion by GSK-3β inhibitors. Previous studies have demonstrated that GSK-3β inhibitors promote cell cycle progression and increase its phosphorylation (19, 28, 31). Since the *Epm2a* mutation has the same effect, it is of great interest to determine if the underlying mechanism is the same. We treated primary WT and *Epm2a*$^{-/-}$ MEF with two GSK-3 inhibitors for 48 h. The viable cells were measured by MTT assay. As shown in Fig. 7a, both LiCl and BIO significantly increased the number of viable WT cells in 48 h, as reported by others (19, 28, 31). As expected, targeted mutation of *Epm2a* also increased cell growth. However, the *Epm2a*$^{-/-}$ MEF no longer responded to the inhibitors. Likewise, the increased accumulation of cyclin D1 was also abrogated by targeted mutation of *Epm2a*. These data are consistent with the notion that the effect of *Epm2a* mutation on cell cycle progression is explained by inhibition of GSK-3β activity.

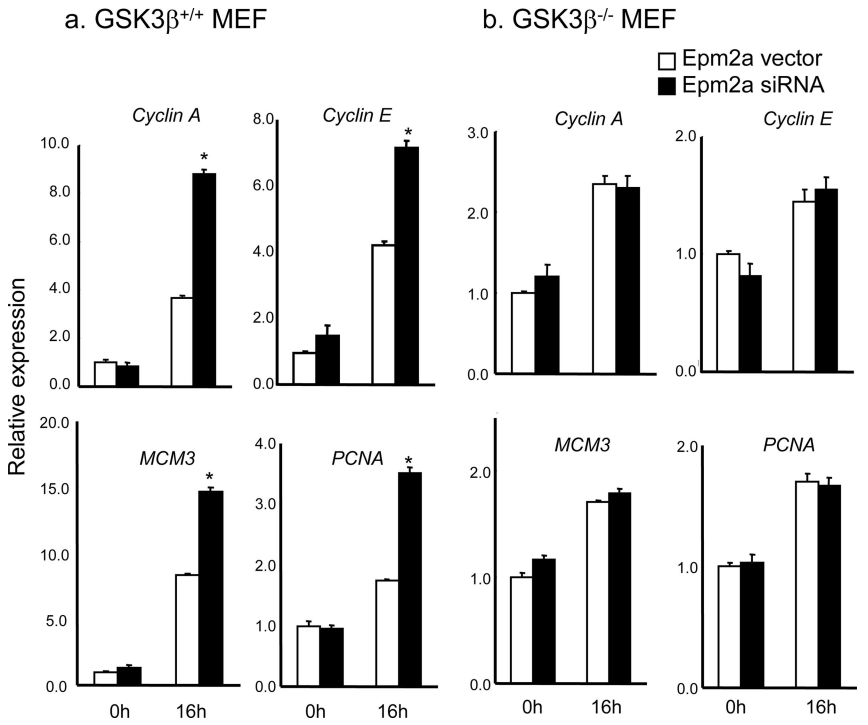

FIG. 6. Laforin downregulates the transcription of E2F and TCF/LEF target genes in GSK-3β$^{+/+}$ MEF (a) but not GSK-3β$^{-/-}$ MEF (b). The mRNA levels of these target genes were measured by real-time PCR. The mRNA was extracted from *Epm2a*-silenced and control cells, with 10% FBS stimulation for 16 h after serum starvation for 24 h (0 h). *Hprt* was used as an internal control. Data shown are means ± SD from triplicates and are representative of three independent experiments. *, $P < 0.05$.

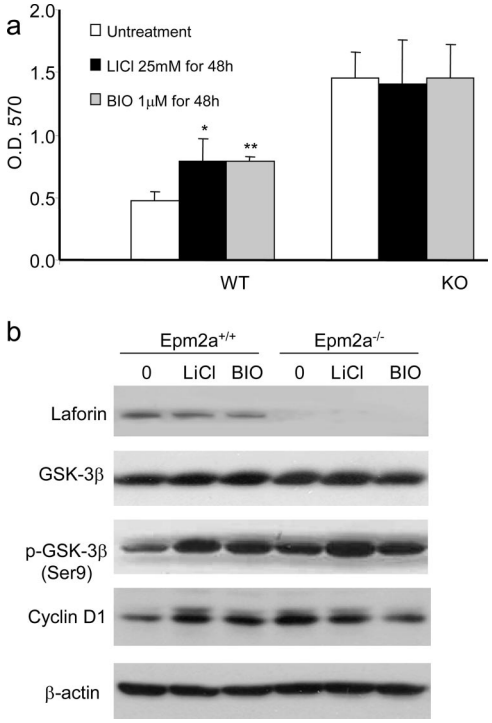

FIG. 7. The effect of GSK-3β inhibitors on cell cycle progression of WT and *Epm2a*$^{-/-}$ MEF. MEF from *Epm2a* WT and knockout (KO) mice were incubated with two GSK3β inhibitors, LiCl and BIO, for 48 h, followed by MTT assay (a) and Western blotting (b). (a) Data are means ± SD of results for three mice in each group. The testing of these data was repeated twice. O.D. 570, optical density at 570 nm. *, $P < 0.05$; **, $P < 0.01$.

DISCUSSION

We have previously demonstrated that insertional mutation and epigenetic silencing of the *Epm2a* gene led to the development of T lymphoma in transgenic mice with limited T-cell immunity (32). These data suggest that *Epm2a* is a novel tumor suppressor in immunocompromised hosts. The current study explores the molecular mechanism by which laforin suppresses cell growth under physiological conditions.

The data in this report demonstrated that silencing *Epm2a* by either siRNA or targeted mutation increased the growth rate in three independent models, including ex vivo thymocytes, primary culture of untransformed MEF, and immortalized MEF. The increased growth rate is associated with increased cyclin D1 function, such as the phosphorylation of Rb and the upregulation of Rb-targeted genes. Importantly, the *Epm2a* function depends on functional GSK-3β, as the effect is completely abrogated in GSK-3β$^{-/-}$ MEF. Collectively, these data revealed a missing link between laforin and cell cycle regulation.

It is of interest that laforin deficiency and GSK-3 inhibitors have the same effect on the growth rate of MEF. In addition, the two effects cannot be compounded, as laforin-deficient cells no longer respond to GSK-3 inhibitors. These data are best explained if the basis for increased proliferation in both cases is the same. Surprisingly, while the inhibitors appear to induce the phosphorylation of GSK-3β at Ser9, regardless of the presence of laforin, the impact on the levels of cyclin D1 and cell growth can be observed only if laforin is also present. It appears that in the absence of laforin, the GSK-3 inhibitors

may even reduce the levels of cyclin D1 somewhat. One way that these data can be reconciled is that modulation of GSK-3β activity can be achieved by a laforin-dependent mechanism that is unrelated to the phosphorylation of Ser9. In this regard, it is intriguing that GSK-3β repression of Wnt signaling can be abrogated by the phosphorylation of a C-terminal Ser (30). Alternatively, the impact of GSK-3β inhibition on cell growth may have reached the maximum if laforin is absent. Additional studies are needed to clarify the mechanism.

Theoretically, there are at least two mechanisms by which laforin–GSK-3β regulates the levels of cyclin D1. First, as a positive regulator of GSK-3β activity (17, 32), laforin can negatively regulate Wnt signaling, as we have reported previously (32). Since the dominant negative mutant of TCF prevented the increase of the cyclin D1 transcript, we suggest that the negative regulation of cyclin D1 mRNA levels by laforin is mediated by Wnt signaling (see Fig. S3 in the supplemental material). In addition, since GSK-3β is known to regulate the levels of cyclin D1 by direct phosphorylation (3, 7), it is plausible that by modulating GSK-3β activity, laforin regulates the stability of cyclin D1.

ACKNOWLEDGMENTS

We thank Christopher J. Phiel from Columbus Children's Hospital for the MEF used in the study and Lynde Shaw and Todd Brown for secretarial assistance.

This study is supported by grants from the American Cancer Society (P.Z.), the U.S. Department of Defense (P.Z.), the National Institutes of Health (Y.L.), and the Canadian Institutes of Health Research (B.A.M.).

REFERENCES

1. **Aberle, H., A. Bauer, J. Stappert, A. Kispert, and R. Kemler.** 1997. Beta-catenin is a target for the ubiquitin-proteasome pathway. EMBO J. **16:**3797–3804.
2. **Ali, A., K. P. Hoeflich, and J. R. Woodgett.** 2001. Glycogen synthase kinase-3: properties, functions, and regulation. Chem. Rev. **101:**2527–2540.
3. **Alt, J. R., J. L. Cleveland, M. Hannink, and J. A. Diehl.** 2000. Phosphorylation-dependent regulation of cyclin D1 nuclear export and cyclin D1-dependent cellular transformation. Genes Dev. **14:**3102–3114.
4. **Behrens, J., B. A. Jerchow, M. Wurtele, J. Grimm, C. Asbrand, R. Wirtz, M. Kuhl, D. Wedlich, and W. Birchmeier.** 1998. Functional interaction of an axin homolog, conductin, with beta-catenin, APC, and GSK3beta. Science **280:**596–599.
5. **Chan, E. M., C. A. Ackerley, H. Lohi, L. Ianzano, M. A. Cortez, P. Shannon, S. W. Scherer, and B. A. Minassian.** 2004. Laforin preferentially binds the neurotoxic starch-like polyglucosans, which form in its absence in progressive myoclonus epilepsy. Hum. Mol. Genet. **13:**1117–1129.
6. **Cohen, P., and S. Frame.** 2001. The renaissance of GSK3. Nat. Rev. Mol. Cell Biol. **2:**769–776.
7. **Diehl, J. A., M. Cheng, M. F. Roussel, and C. J. Sherr.** 1998. Glycogen synthase kinase-3beta regulates cyclin D1 proteolysis and subcellular localization. Genes Dev. **12:**3499–3511.
8. **Durbin, J. E., R. Hackenmiller, M. C. Simon, and D. E. Levy.** 1996. Targeted disruption of the mouse Stat1 gene results in compromised innate immunity to viral disease. Cell **84:**443–450.
9. **Ewen, M. E., H. K. Sluss, C. J. Sherr, H. Matsushime, J. Kato, and D. M. Livingston.** 1993. Functional interactions of the retinoblastoma protein with mammalian D-type cyclins. Cell **73:**487–497.
10. **Ganesh, S., K. L. Agarwala, K. Ueda, T. Akagi, K. Shoda, T. Usui, T. Hashikawa, H. Osada, A. V. Delgado-Escueta, and K. Yamakawa.** 2000. Laforin, defective in the progressive myoclonus epilepsy of Lafora type, is a dual-specificity phosphatase associated with polyribosomes. Hum. Mol. Genet. **9:**2251–2261.
11. **Ganesh, S., A. V. Delgado-Escueta, T. Sakamoto, M. R. Avila, J. Machado-Salas, Y. Hoshii, T. Akagi, H. Gomi, T. Suzuki, K. Amano, K. L. Agarwala, Y. Hasegawa, D. S. Bai, T. Ishihara, T. Hashikawa, S. Itohara, E. M. Cornford, H. Niki, and K. Yamakawa.** 2002. Targeted disruption of the Epm2a gene causes formation of Lafora inclusion bodies, neurodegeneration, ataxia, myoclonus epilepsy and impaired behavioral response in mice. Hum. Mol. Genet. **11:**1251–1262.
12. **Grimes, C. A., and R. S. Jope.** 2001. The multifaceted roles of glycogen synthase kinase 3beta in cellular signaling. Prog. Neurobiol. **65:**391–426.
13. **Guan, K. L., C. W. Jenkins, Y. Li, M. A. Nichols, X. Wu, C. L. O'Keefe, A. G. Matera, and Y. Xiong.** 1994. Growth suppression by p18, a p16INK4/MTS1- and p14INK4B/MTS2-related CDK6 inhibitor, correlates with wild-type pRb function. Genes Dev. **8:**2939–2952.
14. **Guan, K. L., C. W. Jenkins, Y. Li, C. L. O'Keefe, S. Noh, X. Wu, M. Zariwala, A. G. Matera, and Y. Xiong.** 1996. Isolation and characterization of p19INK4d, a p16-related inhibitor specific to CDK6 and CDK4. Mol. Biol. Cell **7:**57–70.
15. **Hoeflich, K. P., J. Luo, E. A. Rubie, M. S. Tsao, O. Jin, and J. R. Woodgett.** 2000. Requirement for glycogen synthase kinase-3beta in cell survival and NF-kappaB activation. Nature **406:**86–90.
16. **Leone, G., J. DeGregori, Z. Yan, L. Jakoi, S. Ishida, R. S. Williams, and J. R. Nevins.** 1998. E2F3 activity is regulated during the cell cycle and is required for the induction of S phase. Genes Dev. **12:**2120–2130.
17. **Lohi, H., L. Ianzano, X. C. Zhao, E. M. Chan, J. Turnbull, S. W. Scherer, C. A. Ackerley, and B. A. Minassian.** 2005. Novel glycogen synthase kinase 3 and ubiquitination pathways in progressive myoclonus epilepsy. Hum. Mol. Genet. **14:**2727–2736.
18. **Matsushime, H., M. E. Ewen, D. K. Strom, J. Y. Kato, S. K. Hanks, M. F. Roussel, and C. J. Sherr.** 1992. Identification and properties of an atypical catalytic subunit (p34PSK-J3/cdk4) for mammalian D type G1 cyclins. Cell **71:**323–334.
19. **Meijer, L., A. L. Skaltsounis, P. Magiatis, P. Polychronopoulos, M. Knockaert, M. Leost, X. P. Ryan, C. A. Vonica, A. Brivanlou, R. Dajani, C. Crovace, C. Tarricone, A. Musacchio, S. M. Roe, L. Pearl, and P. Greengard.** 2003. GSK-3-selective inhibitors derived from Tyrian purple indirubins. Chem. Biol. **10:**1255–1266.
20. **Minassian, B. A., D. M. Andrade, L. Ianzano, E. J. Young, E. Chan, C. A. Ackerley, and S. W. Scherer.** 2001. Laforin is a cell membrane and endoplasmic reticulum-associated protein tyrosine phosphatase. Ann. Neurol. **49:**271–275.
21. **Minassian, B. A., L. Ianzano, M. Meloche, E. Andermann, G. A. Rouleau, A. V. Delgado-Escueta, and S. W. Scherer.** 2000. Mutation spectrum and predicted function of laforin in Lafora's progressive myoclonus epilepsy. Neurology **55:**341–346.
22. **Minassian, B. A., J. R. Lee, J. A. Herbrick, J. Huizenga, S. Soder, A. J. Mungall, I. Dunham, R. Gardner, C. Y. Fong, S. Carpenter, L. Jardim, P. Satishchandra, E. Andermann, O. C. Snead III, I. Lopes-Cendes, L. C. Tsui, A. V. Delgado-Escueta, G. A. Rouleau, and S. W. Scherer.** 1998. Mutations in a gene encoding a novel protein tyrosine phosphatase cause progressive myoclonus epilepsy. Nat. Genet. **20:**171–174.
23. **Narita, M., S. Nunez, E. Heard, A. W. Lin, S. A. Hearn, D. L. Spector, G. J. Hannon, and S. W. Lowe.** 2003. Rb-mediated heterochromatin formation and silencing of E2F target genes during cellular senescence. Cell **113:**703–716.
24. **Serrano, M., G. J. Hannon, and D. Beach.** 1993. A new regulatory motif in cell-cycle control causing specific inhibition of cyclin D/CDK4. Nature **366:**704–707.
25. **Sherr, C. J.** 2004. Principles of tumor suppression. Cell **116:**235–246.
26. **Sherr, C. J., and F. McCormick.** 2002. The RB and p53 pathways in cancer. Cancer Cell **2:**103–112.
27. **Sherr, C. J., and J. M. Roberts.** 1999. CDK inhibitors: positive and negative regulators of G1-phase progression. Genes Dev. **13:**1501–1512.
28. **Sinha, D., Z. Wang, K. L. Ruchalski, J. S. Levine, S. Krishnan, W. Lieberthal, J. H. Schwartz, and S. C. Borkan.** 2005. Lithium activates the Wnt and phosphatidylinositol 3-kinase Akt signaling pathways to promote cell survival in the absence of soluble survival factors. Am. J. Physiol. Renal Physiol. **288:**F703–F713.
29. **Stacey, D. W.** 2003. Cyclin D1 serves as a cell cycle regulatory switch in actively proliferating cells. Curr. Opin. Cell Biol. **15:**158–163.
30. **Thornton, T. M., G. Pedraza-Alva, B. Deng, C. D. Wood, A. Aronshtam, J. L. Clements, G. Sabio, R. J. Davis, D. E. Matthews, B. Doble, and M. Rincon.** 2008. Phosphorylation by p38 MAPK as an alternative pathway for GSK3beta inactivation. Science **320:**667–670.
31. **Tseng, A. S., F. B. Engel, and M. T. Keating.** 2006. The GSK-3 inhibitor BIO promotes proliferation in mammalian cardiomyocytes. Chem. Biol. **13:**957–963.
32. **Wang, Y., Y. Liu, C. Wu, H. Zhang, X. Zheng, Z. Zheng, T. L. Geiger, G. J. Nuovo, Y. Liu, and P. Zheng.** 2006. Epm2a suppresses tumor growth in an immunocompromised host by inhibiting Wnt signaling. Cancer Cell **10:**179–190.
33. **Xiong, Y., T. Connolly, B. Futcher, and D. Beach.** 1991. Human D-type cyclin. Cell **65:**691–699.
34. **Xiong, Y., H. Zhang, and D. Beach.** 1993. Subunit rearrangement of the cyclin-dependent kinases is associated with cellular transformation. Genes Dev. **7:**1572–1583.